CrossMark

Thermal energy storage and retrieval properties of form-stable phase change nanofibrous mats based on ternary fatty acid eutectics/polyacrylonitrile composite by magnetron sputtering of silver

Huizhen Ke[1] · Zengyuan Pang[1] · Bin Peng[1] · Jing Wang[1] · Yibing Cai[1] ·
Fenglin Huang[1] · Qufu Wei[1]

Abstract This paper demonstrated a novel magnetron sputtering method used for the improvement in thermal energy storage and retrieval rates of phase change materials (PCMs). The ten types of ternary fatty acid eutectics (i.e., CA–LA–MA, CA–LA–PA, CA–LA–SA, CA–MA–PA, CA–MA–SA, CA–PA–SA, LA–MA–PA, LA–MA–SA, LA–PA–SA and MA–PA–SA) were firstly prepared using five fatty acids such as capric acid (CA), lauric acid (LA), myristic acid (MA), palmitic acid (PA) and stearic acid (SA) and then selected as solid–liquid PCMs. Thereafter, magnetron sputter coating was used to deposit the functional silver (Ag) nanolayers onto the surface of electrospun polyacrylonitrile (PAN) nanofibrous mats serving as supporting skeleton. Finally, a series of composite PCMs were fabricated by adsorbing the prepared ternary eutectics into three-dimensional porous network structures of Ag-coated PAN membranes. The observations by EDX determined the formation of Ag nanolayers on the PAN nanofibers surface after magnetron sputtering. The SEM images illustrated that the Ag-coated PAN nanofibers appeared to have larger fiber diameter and rougher surface. Ag-coated PAN nanofibrous mats could effectively prevent the leakage of molten ternary eutectics and help maintain form-stable structure due to surface tension forces, capillary and nanoconfinement effects. The DSC results suggested that the phase change temperatures of the ternary fatty acid eutectics were obviously lower than those of individual fatty acids and their binary eutectics. The adsorption rates of ternary fatty acid eutectics in the composite PCMs were determined to be about 89–98 %. The thermal performance test indicated that the metallic coating of Ag dramatically improved the thermal energy storage and retrieval rates of the composite PCMs.

Keywords Thermal storage and retrieval rates · Phase change nanofibrous mats · Ternary fatty acid eutectics · Sputter coating of silver · Thermal properties

Introduction

Energy issue is a global problem, which is significantly influencing and threatening sustainable development and survival of human beings. Obviously, the development of renewable energy sources and improvement in efficiency of energy systems are two solutions to address this problem. Thermal energy storage and release materials are attracting increasing attentions. Among these materials, phase change materials (PCMs) have been widely studied and successfully applied in a wide range of latent heat storage systems and temperature control applications such as solar water heaters, concentrating solar power, building energy conservation systems, heat storage condensers, vehicle thermal buffer, Li-ion batteries, heat management of electronics, agricultural temperature-adaptable greenhouses, homothermal clothing, smart air-conditioning systems, industrial waste heat recovery systems, medical applications, telecommunications and microprocessor equipment due to their desirable characteristics like high energy storage density, small temperature variation during phase change processes, lower vapor pressure and volume change [1–12].

A wide variety of organic PCMs (e.g., paraffins, fatty acids, fatty acid esters, glycols and alcohols), inorganic

✉ Qufu Wei
qfwei@jiangnan.edu.cn

[1] Key Laboratory of Eco-Textiles, Ministry of Education, Jiangnan University, Wuxi 214122, Jiangsu, China

🗍 Springer

PCMs (e.g., salt hydrates, metals) and eutectic PCMs (e.g., binary or ternary fatty acid eutectics) have been extensively investigated during recent several decades. Fatty acids are one of the most efficient solid–liquid PCMs for thermal energy storage owing to their prominent advantages, e.g., outstanding thermal properties, excellent thermal and chemical stability, high phase change enthalpies, suitable phase change temperatures, non-toxicity, non-corrosiveness, no supercooling and phase segregation, self-nucleating behavior, recyclable and low cost [13–15]. Moreover, fatty acids are more sustainable than other PCMs and can provide an assurance of continuous supply despite the shortage of fuel sources because they are easily obtained from common vegetables and animal oils. Although fatty acids exhibit a host of superior properties, phase transition temperatures of fatty acids are much higher than temperatures of actual climatic requirement. As a result of it, their applications are significantly limited by this characteristic drawback. According to the lowest eutectic point theory, the phase change temperatures of fatty acids could be regulated to suitable values with their phase change enthalpies maintaining the high values by adjusting the composition and mass ratio of fatty acid in their eutectic mixtures. The previous literatures and our researches have verified that fatty acid eutectics can be considered as potential PCMs for the related application of thermal energy storage and retrieval [13–15].

However, the leakage and poor thermal conductivity of fatty acid eutectics have seriously hindered their direct applications in many fields. Therefore, form-stable PCMs with improved thermal conductivity performances have been rapidly exploited to solve these problems. Currently, various polymers and inorganic materials have been selected as supporting materials to fabricate form-stable PCMs such as high-density polyethylene [16], high-density polyethylene–ethylene–vinyl acetate [17], polyaniline [18], polyamide 6 [19], polyethylene terephthalate [20], titania [21], activated carbon [22], montmorillonite [23], diatomite [24], silicon dioxide [25] and expanded perlite [26]. Additionally, thermal conductivity of form-stable PCMs can be significantly improved by adding some inorganic materials with desirable thermal conductivity including graphene nanoplatelets [27] and expanded graphite [28] into the phase change systems. In spite of these materials, incorporating into form-stable PCMs can greatly enhance thermal conductivity of phase change systems during phase change processes, and they are normally difficult to disperse in the systems resulting in the limitation of additive amounts.

Magnetron sputter coating is a promising physical vapor deposition (PVD) technique. It is performed by employing a high voltage across a low-pressure gas to create plasma, which consists of electrons and gas ions in a high energy state. During sputter coating, energized gas ions strike a target, composed of the desired coating material, and cause atoms from the target to be knocked off with high energy to travel to and bond with the substrate, forming a thin film on the surface of the substrate [29, 30]. Compared to other approaches used to improve the thermal conductivity of PCMs, sputter coating provides a new environmental friendly technique with such advantages as uniform and compact deposition, strong bonding between coating of heat conduction and phase change systems, simple operation, high productivity, low cost and suitability for industrial production. Therefore, this method can be considered to deposit very thin functional metallic coatings with high thermal conductivity on various PCMs or supporting materials of form-stable PCMs for improving the thermal conductivity of the PCMs systems.

However, to the best of our knowledge, there have been no reports about enhancement of thermal energy storage and release rates of form-stable PCMs by using magnetron sputter coating technology. Additionally, it was well known that electrospun polymer nanofibers can be selected as preferred supporting materials for the preparation of form-stable PCMs due to the unique characteristics of large surface-to-volume ratio, flexibility, light weight and porous network structure with the desired level of openness [31, 32]. Moreover, the studies on form-stable composite PCMs with ternary fatty acid eutectics being adsorbed and/or encapsulated in metal-coated polymer nanofibrous mats with excellent thermal conductivity through physical absorption have not been reported.

Therefore, the objective of this study was to adopt the novel magnetron sputtering method to improve the heat transfer efficiencies of form-stable composite PCMs. The series of innovative ternary fatty acid eutectics with suitable phase change temperatures and high latent heat values including CA–LA–MA, CA–LA–PA, CA–LA–SA, CA–MA–PA, CA–MA–SA, CA–PA–SA, LA–MA–PA, LA–MA–SA, LA–PA–SA and MA–PA–SA, which can be used as lower-temperature solid–liquid PCMs for application related to thermal energy storage and release, were first prepared and evaluated. Thereafter, the Ag-coated polyacrylonitrile (PAN) nanofibrous mats with excellent thermal conductivity, high porosity and three-dimensional network structure were exploited as supporting materials to adsorb the prepared ternary fatty acid eutectics by physical absorption method. The surface chemical structures, morphologies, phase change behaviors, thermal reliability, heat energy storage and release rates of the uncoated and Ag-coated ternary fatty acid eutectics/PAN composite PCMs were systematically investigated by EDX, FT-IR, SEM, DSC and measurement of melting/freezing times, respectively.

Experimental

Materials

The powder of polyacrylonitrile (PAN, $M_w = 150,000$) was purchased from Aldrich. The chemicals of capric acid (CA), lauric acid (LA), myristic acid (MA), palmitic acid (PA), stearic acid (SA) and N,N-dimethyl formamide (DMF) were supplied by the Sinopharm Group Chemical Reagent Co., Ltd. (Shanghai, China). All of the chemicals were used as received without further purifications.

Electrospinning

The 10 mass% PAN powder was dissolved in DMF solvent, and magnetic stirring was applied to form homogeneous solution. The electrospinning setup consisted of a high voltage power supply, purchased from the Dongwen Co. (Tianjing, China), and a syringe pump, purchased from the Medical Instrument Co. (Hangzhou, China), as well as a nanofiber collector of laboratory-produced roller with diameter of 25 cm. During electrospinning, the rotating speed of the roller was fixed at 100 rpm. The voltage applied and the distance between needle tip and roller collector were set at 18 kV and 16 cm, respectively. The solution feed rate was maintained at 0.5 mL h^{-1}. The electrospun PAN nanofibers were collected as overlaid fibrous membranes and dried in a vacuum oven at room temperature for 24 h to remove the residual solvent.

Magnetron sputter coating

A magnetron sputter coating system supplied by Shenyang Juzhi, Ltd., was used to deposit the Ag nanolayers on the surface of electrospun PAN nanofibrous mats at room temperature, as illustrated in Fig. 1. A high-purity Ag target (99.999 %) was mounted on the cathode, and the PAN nanofibrous mats were placed on the anode with a side
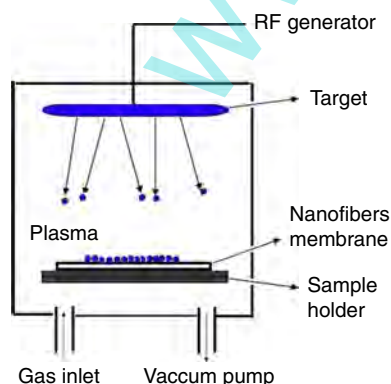

Fig. 1 Schematic diagrams of sputter coating

facing the target. The sputtering pressure was adjusted to 0.5 Pa using the bombardment gas of argon (99.999 %). The coatings were performed on both sides of sample using radio frequency (RF) sputter coating with the power of 90 W for 2 h per side. The sample holder with a rotation speed of 100 rpm was introduced to improve the uniformity of the deposition on electrospun PAN nanofibrous mats.

Preparation of ternary fatty acid eutectics

Calculation of eutectic mass ratios

In this work, the Schrader equation was used to calculate the theoretical eutectic mass ratios of ternary fatty acid mixtures [19].

$$T = 1/\left(1/T_f - R\ln X_A/\Delta_s^1 H_A\right) \qquad (1)$$

where T (K) is the melting temperature of the mixture containing compound A, X_A is the mole fraction of component A in the mixture, $\Delta_s^1 H_A$ (J mol^{-1}) and T_f (K) are the melting enthalpy and melting temperature of compound A, and R is the gas constant (8.314 J K^{-1} mol^{-1}). It necessary to account for that T_f (K) used in this paper is the T_e (°C) listed in Tables 1 and 2. It is notable that the Celsius scale should be transformed into Fahrenheit scale. Moreover, the experimentally determined eutectic mass ratios of fatty acid mixtures modestly deviated from the theoretical values because of the small amounts of impurities in fatty acids and experimental errors associated with DSC analyses, resulting in the fact that the actual eutectic mass ratios of ternary fatty acid mixtures need to be determined based on both calculated and experimental results. Table 3 reveals the experimentally determined eutectic mass ratios of ternary fatty acid eutectics.

Preparation process of ternary fatty acid eutectics

The ternary fatty acid eutectics were prepared through melt-blending followed by ultrasonication [19]. Based on the experimentally determined eutectic mass ratios, the selected fatty acids were first added into a beaker and then placed into an oven at 60 °C for 2 h. Thereafter, the beaker with the molten ternary fatty acid eutectics was put in a 330-W ultrasonic water bath at 60 °C for 2 min, and finally, the ternary fatty acid eutectics were obtained for the following studies.

Size stability measurement of Ag-coated fibrous membranes

In order to verify the size stability of Ag-coated PAN fibrous membranes in phase change temperature conditions, the Ag-

Table 1 Peak onset temperature (T_e), melting peak temperature (T_m), freezing peak temperature (T_c), melting enthalpy (ΔH_m) and freezing enthalpy (ΔH_c) of the five fatty acids

Fatty acids	Melting			Freezing		
	T_e/°C	T_m/°C	ΔH_m/kJ kg^{-1}	T_e/°C	T_c/°C	ΔH_c/kJ kg^{-1}
CA	31.12	32.71	166.7	29.30	29.25	163.1
LA	44.02	44.63	182.3	42.09	41.73	182.4
MA	53.73	56.06	187.3	52.09	51.94	184.9
PA	62.11	64.83	212.1	60.38	59.28	214.6
SA	68.96	70.52	222.8	67.06	66.50	226.7

Table 2 Peak onset temperature (T_e), melting peak temperature (T_m), freezing peak temperature (T_c), melting enthalpy (ΔH_m) and freezing enthalpy (ΔH_c) of the ten binary fatty acid eutectics

Binary fatty acid eutectics	Eutectic mass ratios	Melting			Freezing		
		T_e/°C	T_m/°C	ΔH_m/kJ kg^{-1}	T_e/°C	T_c/°C	ΔH_c/kJ kg^{-1}
CA–LA	66.75/33.25	19.26	22.70	127.2	18.41	16.43	125.2
CA–MA	78.39/21.61	20.08	26.02	155.2	17.07	15.08	145.9
CA–PA	89/11	22.90	28.71	141.4	20.39	19.26	136.1
CA–SA	94.47/5.53	25.71	31.17	156.8	23.61	22.94	147.1
LA–MA	61.27/38.73	33.27	36.75	173.6	33.71	31.88	168.0
LA–PA	77.51/22.49	33.60	36.52	169.6	31.22	30.31	168.3
LA–SA	87.24/12.76	37.98	41.73	181.2	33.77	32.25	166.5
MA–PA	66.92/33.08	45.36	47.39	183.1	43.80	42.20	185.6
MA–SA	77.42/22.58	46.41	48.37	180.6	42.09	41.17	177.3
PA–SA	62.99/37.01	53.69	56.16	204.7	53.45	52.43	204.2

Table 3 Peak onset temperature (T_e), melting peak temperature (T_m), freezing peak temperature (T_c), melting enthalpy (ΔH_m) and freezing enthalpy (ΔH_c) of the ten ternary fatty acid eutectics

Ternary fatty acid eutectics	Eutectic mass ratios	Melting			Freezing		
		T_e/°C	T_m/°C	ΔH_m/kJ kg^{-1}	T_e/°C	T_c/°C	ΔH_c/kJ kg^{-1}
CA–LA–MA	66.35/20.62/13.03	15.83	18.72	131.4	13.39	11.14	129.7
CA–LA–PA	63.37/31.56/5.07	15.47	20.75	134	15.38	11.95	132.5
CA–LA–SA	65.32/32.54/2.14	17.85	22.80	132.5	16.92	13.10	129.7
CA–MA–PA	71.82/18.86/9.32	17.56	22.31	136.8	15.22	12.83	132.6
CA–MA–SA	72.65/21.17/6.18	18.93	24.04	145.9	15.66	13.63	143.1
CA–PA–SA	83.82/10.19/5.99	19.72	25.12	145.7	17.64	15.60	144.5
LA–MA–PA	63.32/24.55/12.13	30.82	33.78	155.7	29.52	27.39	154.1
LA–MA–SA	61.02/30.06/8.92	29.21	32.76	152.9	28.70	26.57	153.8
LA–PA–SA	72.26/20.97/6.77	32.02	36.79	159.0	30.29	28.46	159.5
MA–PA–SA	56.82/28.08/15.1	46.69	49.23	170.3	43.45	40.42	168.7

coated fibrous membranes with sizes of 5 cm × 5 cm were placed into an oven at 60 °C for 24 h. And then the size and morphological structure of original and heat-treated Ag-coated PAN fibrous membranes were measured by ruler and then characterized by SEM.

Fabrication of form-stable phase change composite nanofibrous mats

A series of ternary fatty acid eutectics/PAN and ternary fatty acid eutectics/PAN/Ag form-stable composite PCMs were

prepared by physical adsorption. The prepared ternary fatty acid eutectics were first placed in the beakers. The beakers were sealed with the plastic wrap and placed into the constant temperature water bath at 60 °C until eutectic mixtures completely melted. The electrospun PAN nanofibrous mats were cut into samples with sizes of 5 cm × 5 cm. Subsequently, the nanofibrous mats were immersed into molten ternary fatty acid eutectics for 24 h until saturated absorption. Thereafter, the nanofibrous mats absorbed with ternary fatty acid eutectics were hung in an oven at 60 °C for 10 h. Finally, the samples were cooled down to the room temperature for characterization. The codes of samples were referred to as CA–LA–MA/PAN/Ag, CA–LA–PA/PAN/Ag, CA–LA–SA/PAN/Ag, CA–MA–PA/PAN/Ag, CA–MA–SA/PAN/Ag, CA–PA–SA/PAN/Ag, LA–MA–PA/PAN/Ag, LA–MA–SA/PAN/Ag, LA–PA–SA/PAN/Ag and MA–PA–SA/PAN/Ag, respectively.

Characterizations

Energy dispersive X-ray analysis

The electrospun PAN nanofibrous mats before and after sputter coating of Ag were analyzed by EDX analysis at an accelerating voltage of 20 kV with accounting time of 100 s.

FTIR spectroscopy

FTIR spectra were measured using a Nicolet iS10 FT-IR spectrometer over the frequency range of 400–4000 cm^{-1}.

Scanning electron microscopy

The morphological structures of all samples were investigated by a Hitachi SU 1510 SEM. Prior to examination, the all samples except the Ag-coated PAN nanofibrous mats were gold sputter-coated under argon atmosphere to render them electrically conductive.

Atomic force microscopy

A Benyuan CSPM 5000 AFM was employed to image the morphology of the uncoated and Ag-coated electrospun PAN nanofibers. Scanning was carried out in tapping mode AFM, and all samples were scanned at room temperature in atmosphere.

Differential scanning calorimetry

The DSC analyses were carried out using a DSC-Q200 thermal analyzer. The samples were scanned at 8 °C min^{-1}

from −20 to 80 °C. The nitrogen gas flow rate was set at 50 mL min^{-1}. And the 100 times DSC thermal cycling test was also performed to investigate thermal reliability of CA–LA–MA/PAN/Ag form-stable composite PCMs.

Thermal performance test

In order to study the influence of sputtered Ag nanolayers on heat storage and retrieval rates of composite PCMs, thermal performance test was conducted using the experimental setup as our previous work [19, 33]. The all samples were first cut into pieces and put into sealed glass bottles. The amounts of tested samples were about 10 g. Thereafter, the thermocouple was embedded in the center of the test bottle to monitor the difference of time between samples in the same internal temperature. Subsequently, the test bottles were placed into a constant temperature water bath at 40 °C for heat storage process. After this process, the test bottles were rapidly placed in refrigerator at a constant temperature of −10 °C, where the from-stable composite PCMs performed process of heat retrieval. The temperature variations of all samples during heat storage and retrieval processes were automatically recorded by computer via data logger with a temperature measuring accuracy of ±2 °C at time intervals of 1 min. The conductivity measurements were repeated three times.

Results and discussion

EDX analysis

In order to confirm that Ag nanoparticles are really presented on the surface of electrospun PAN nanofibers, SEM-EDX analysis was utilized to determine the chemical compositions of the PAN nanofibrous mats before and after sputter coating of Ag. The EDX spectra of samples are presented in Fig. 2. It can be seen from Fig. 2a, b that the PAN nanofibers dominantly consisted of C, O and N elements before magnetron sputtering, while a large amount of Ag on the surface of PAN nanofibers after magnetron sputter was detected and the amount of C, O, and N was significantly reduced in the EDX spectrum. These results confirmed the formation of the Ag nanolayers on the surface of PAN nanofibers during sputter coating process. Moreover, as shown in Fig. 2c, there were a large amount of C and O elements on the surface of Ag-coated PAN nanofiber membranes after physical adsorption, demonstrating that ternary fatty acid eutectics had also been successfully penetrated into three-dimensional network structure of Ag-coated PAN supporting membranes.

FTIR analysis

The FTIR spectroscopy was used to investigating the chemical compatibility and interaction between ternary fatty acid eutectics and electrospun PAN nanofiber membranes without and with sputter coating of Ag. Figure 3 reveals the typical FTIR spectra of the CA–LA–MA ternary fatty acid eutectics, electrospun PAN nanofibrous mats before and after sputter coating of Ag, as well as uncoated and Ag-coated PAN nanofiber membranes after adsorption of CA–LA–MA ternary fatty acid eutectics. It can be seen from Fig. 3a that the characteristic absorption peaks of CA–LA–MA ternary fatty acid eutectics at around 1707, 1281 and 932 cm^{-1} were ascribed to the stretching vibrations of C=O, C–O and –OH bonds of carboxyl groups, respectively. The asymmetric and symmetric stretching vibrations of C–H bond occurring at the wave numbers of 2922 and 2853 cm^{-1} were also clearly observed from the spectrum, respectively. Moreover, there were two characteristic absorption peaks assigned to the CH$_2$ or CH$_3$

deformation vibration and the rocking vibration in (–CH$_2$–)$_n$ ($n \geq 4$) groups at about 1465 and 721 cm^{-1} in the spectrum, respectively. For the FTIR spectrum of electrospun PAN nanofibrous mats in Fig. 3b, the characteristic absorption peak at about 2242, 2939 and 1452 cm^{-1} was contributed to the stretching vibration of nitrile groups (–C≡N) in PAN molecular chains, as well as the asymmetric and symmetric bending vibrations of methylene groups (–CH$_2$–), respectively [34]. However, the characteristic absorption peaks belonging to PAN molecular in the range of 4000–500 cm^{-1} could not be observed from Fig. 3c, suggesting that the Ag nanolayers had been successfully covered on the surface of electrospun PAN nanofibers during sputter coating process. These results are coincided with the spectrum of EDX analysis. As shown in Fig. 3d, the CA–LA–MA/PAN phase change composite nanofibers obviously exhibited the characteristic absorption peaks of PAN molecular and CA–LA–MA ternary eutectics such as stretching vibration of nitrile groups (–C≡N) at about 2242 cm^{-1} for PAN molecular and the asymmetric and symmetric stretching vibrations of C–H

Fig. 2 EDX spectra of electrospun **a** uncoated and **b** Ag-coated PAN nanofibrous membranes as well as **c** CA–LA–MA/PAN/Ag composite PCM
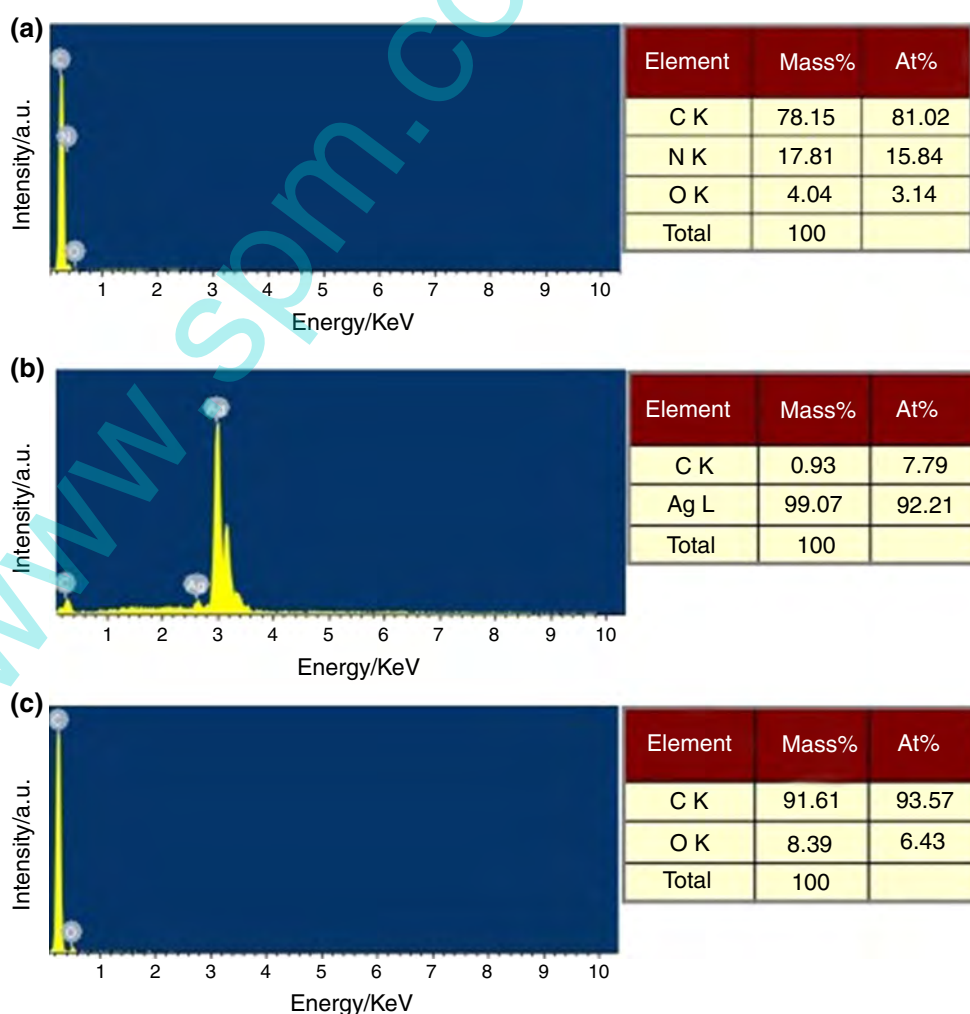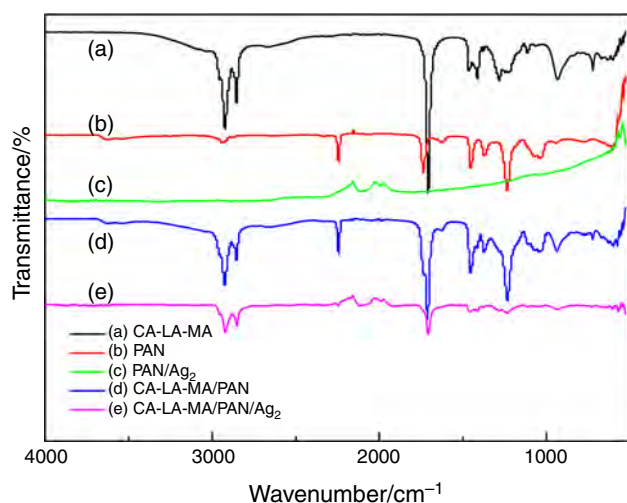
Fig. 3 FTIR spectra of (*a*) CA–LA–MA eutectic, (*b*) uncoated and (*c*) Ag-coated PAN nanofiber membrane, (*d*) CA–LA–MA/PAN composite PCM, as well as (*e*) CA–LA–MA/PAN/Ag$_2$ composite PCM

bond at about 2924 and 2854 cm^{-1} for CA–LA–MA eutectics. No new peaks could be observed from the spectrum of CA–LA–MA/PAN phase change composite nanofibers, which also indicated that there were good chemical compatibility and no chemical reaction between CA–LA–MA eutectics and PAN supporting materials during physical adsorption process. The characteristic absorption peaks in the FTIR spectra of CA–LA–MA/PAN/Ag phase change composite nanofiber membranes were similar to those of CA–LA–MA ternary fatty acid eutectics at the wave numbers of about 2921, 2852 and 1706 cm^{-1} corresponding to the asymmetric and symmetric stretching vibrations of C–H groups, as well as the C=O stretching vibrations as shown in Fig. 3e. These results suggested that the CA–LA–MA ternary fatty acid eutectics were successfully adsorbed into three-dimensional porous network structure of Ag-coated PAN supporting materials.

SEM analysis

The SEM micrographs reveal that the PAN nanofibers formed the porous fibrous network structure during electrospinning, as presented in Fig. 4a. And the neat PAN nanofibers exhibited smooth surfaces, bead-free and cylindrical morphology structures. In comparison with Fig. 4a, obvious differences between uncoated and Ag-coated PAN nanofibers can be observed in Fig. 4b. Surface roughness and average fiber diameter (AFD) of PAN nanofibers significantly increased after sputter coating of Ag. The AFD of uncoated and Ag-coated PAN nanofibers was about 130 and 622 nm, respectively. Figure 4c shows the SEM image of the Ag-coated fibrous membranes after

heating treatment at 60 °C in an oven. It can be found that there was no significant difference about surface structure and fiber diameter between the original Ag-coated PAN nanofibrous membranes and the heat-treated one. And the size of Ag-coated PAN nanofibrous membranes (5 cm × 5 cm) had also not been affected by the increase in ambient temperature from 25 to 60 °C, which meant that Ag-coated PAN nanofibrous membranes have good size stability during the working temperature range of ternary fatty acid eutectics because the glass transition temperature of PAN molecular (about 95 °C) is higher than the phase change temperature of PCMs. It is noted that the both neat PAN nanofibrous mats and Ag-coated PAN nanofibrous mats possessed high surface area-to-volume ratio, three-dimensional structure with highly porous nanofiber network and size stability, so that they can be acted as suitable supporting skeleton to adsorb ternary fatty acid eutectics by physical adsorption. Overall, electrospun PAN nanofibers with the deposition of Ag nanoparticles showed the rougher surface, relative larger fiber diameters and the smaller pore size compared with pristine one.

In order to determine the size of Ag nanoparticles covered on the nanofiber surface, the morphology structure of uncoated and Ag-coated electrospun PAN nanofibers was also characterized by AFM. The typical AFM images of two samples are presented in Fig. 5. The relatively smooth surface of uncoated electrospun PAN nanofibers is clearly observed in Fig. 5a. As shown in Fig. 5b, the growth of the sputtered Ag grains during the sputter coating process led to the formation of compact Ag particles and good coverage of the Ag nanolayer on the electrospun PAN nanofibers. Moreover, the result from the calculation of AFM software reveals that the average size of the sputtered Ag clusters was about 45 nm after the 2 h sputter coating. It was clear that the AFM images sufficiently demonstrated the formation of Ag nanoclusters covered on the PAN nanofiber surface, which was identical to the FE-SEM observation (Fig. 4).

The representative morphological structures of the uncoated and Ag-coated electrospun PAN nanofibrous mats after the adsorption of ternary fatty acid eutectics are shown in Figs. 6 and 7. It can be clearly found that the ternary fatty acid eutectics can easily be dispersed and absorbed into the pores of uncoated and Ag-coated PAN nanofibers supporting matrices to generate the form-stable composite PCMs by the capillary and surface tension forces. The unclear interface structures between nanofibers can also be obviously observed due to the accumulation and adsorption of ternary fatty acid eutectics on the surface of nanofibrous mats. There were no significant differences about morphological structure of from-stable composite PCMs absorbing different types of ternary fatty acid eutectics. It is clear that the uncoated and Ag-coated PAN

Fig. 4 Surface morphology of electrospun PAN nanofibers in SEM: **a** uncoated, **b** Ag-coated and **c** Ag-coated after heat treatment at 60 °C oven
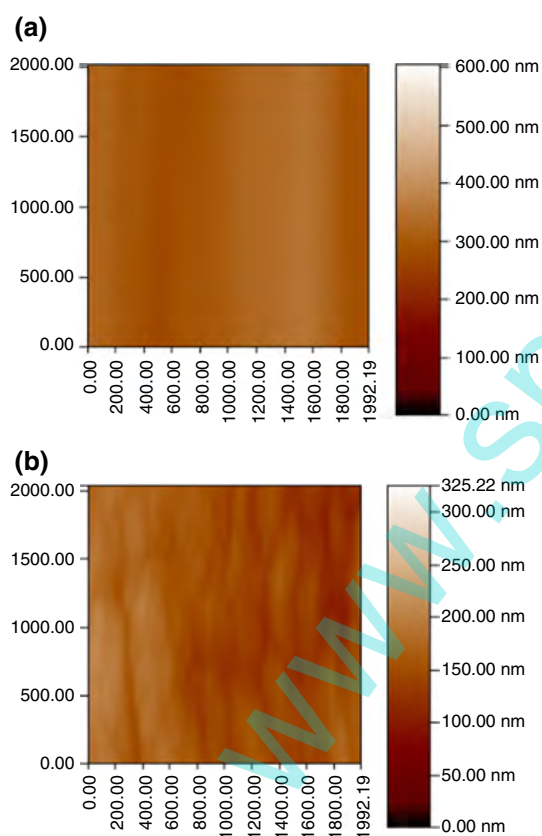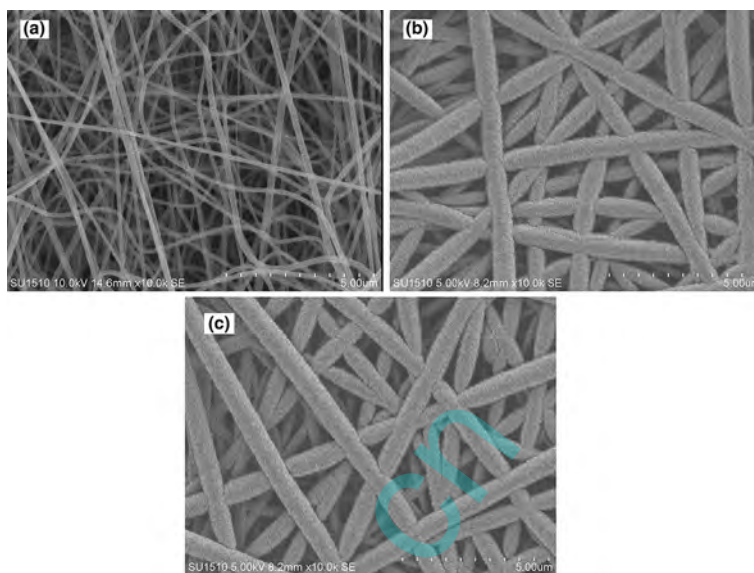

(a)

(b)

Fig. 5 AFM images of electrospun PAN nanofibers: **a** uncoated and **b** Ag-coated

nanofibers could provide the mechanical strength for phase change system and effectively prevent the leakage of molten ternary fatty acid eutectics from the three-dimensional porous network structure of supporting matrices according to the fact that the ternary fatty acid eutectics

could well be encapsulated into pores of nanofibrous mats even if the SEM processing temperature exceeded the melting points of some ternary fatty acid eutectics. The SEM images indicated that the innovative ternary fatty acid eutectics/PAN/Ag form-stable phase change composite nanofibrous mats had been successfully prepared through magnetron sputter of Ag following by the physical adsorption. And the metallic-coated electrospun PAN nanofibrous mats have great potential to act as a new kind of supporting materials for the preparation of form-stable composite PCMs.

Thermal energy storage and release properties of ternary fatty acid eutectics

The DSC curves of individual fatty acids, the prepared binary and ternary fatty acid eutectics during heating and cooling processes are shown in Figs. 8–10. The corresponding thermal characteristic data including peak onset temperature (T_e), melting peak temperature (T_m), freezing peak temperature (T_c), melting enthalpy (ΔH_m) and freezing enthalpy (ΔH_c) are summarized in Tables 1–3. According to Tables 1–3, there were a significant decrease in the phase change temperatures of the prepared ternary fatty acid eutectics in comparison with those of the original individual fatty acids and the prepared binary fatty acid eutectics, which suggested that phase change temperatures of fatty acid eutectics had a gradual reduction trend with the addition of component in the eutectic mixtures. It can be found from Figs. 9 and 10 that all prepared fatty acid eutectics presented only one single endothermic and exothermic peaks during the DSC analyses, demonstrating that the binary and ternary fatty acid eutectics were

Fig. 6 Representative SEM images of form-stable composite PCMs without sputter coating of Ag: **a** CA–LA–MA/PAN, **b** CA–LA–PA/PAN, **c** CA–LA–SA/PAN, **d** CA–MA–PA/PAN, **e** CA–MA–SA/PAN, **f** CA–PA–SA/PAN, **g** LA–MA–PA/PAN, **h** LA–MA–SA/PAN, **i** LA–PA–SA/PAN, and **j** MA–PA–SA/PAN
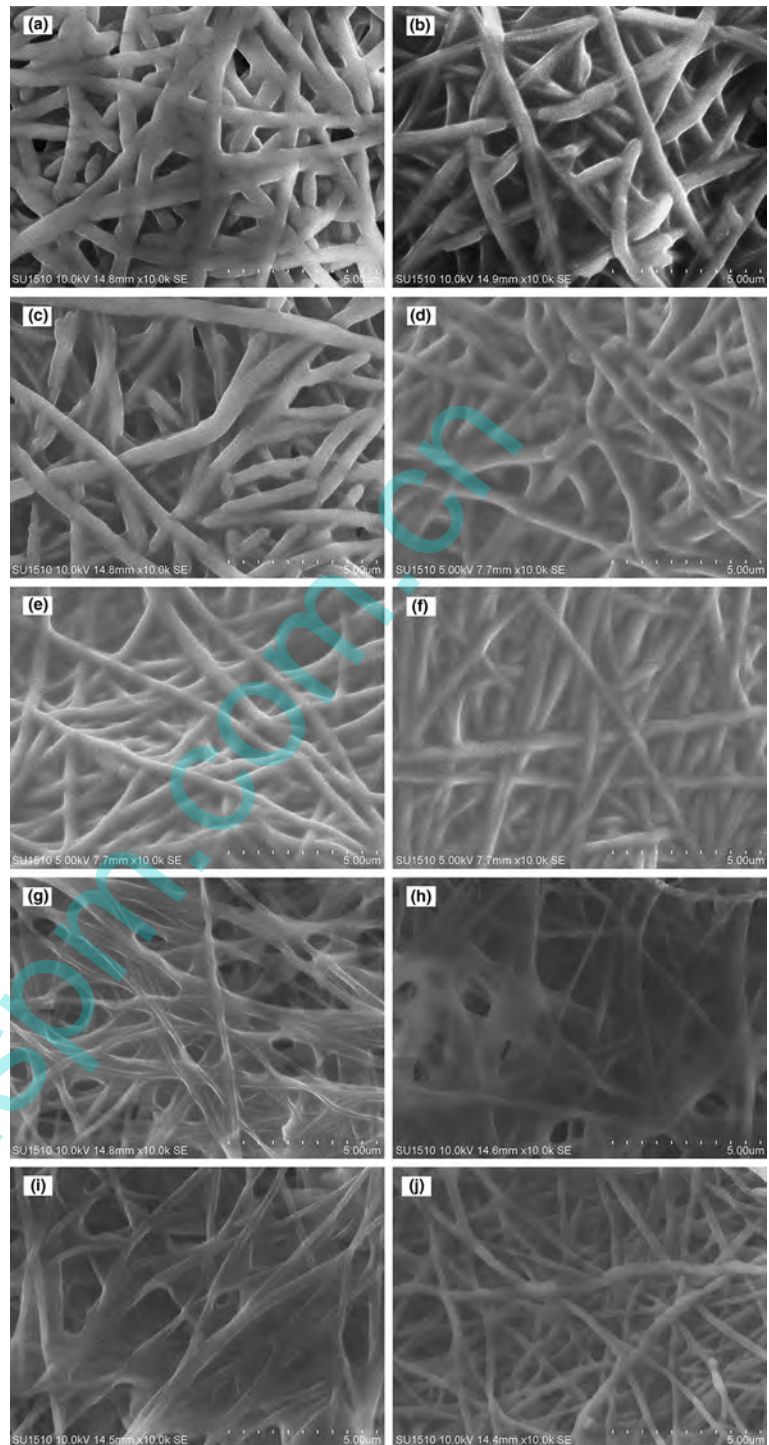
successfully prepared by melt-blending and ultrasonic vibration methods. Moreover, it can be seen from Fig. 10 that the types of fatty acid selecting as ingredient to prepare the ternary fatty acid eutectics had a significant effect on the phase change temperatures and enthalpies of the obtained eutectic mixtures. In other word, the ternary fatty acid eutectics, which were prepared using the individual

fatty acids with the relatively short molecular chain structure, represented a relatively lower phase change temperatures and enthalpies. Figure 10 shows that the prepared different kinds of ternary fatty acid eutectic exhibited different thermal energy storage properties. The T_e and ΔH_m of the prepared ternary fatty acid eutectics ranged from 15.83 to 46.69 °C, and from 131.4 to

Fig. 7 Representative SEM images of form-stable composite PCMs with sputter coating of Ag: **a** CA–LA–MA/PAN/Ag, **b** CA–LA–PA/PAN/Ag, **c** CA–LA–SA/PAN/Ag, **d** CA–MA–PA/PAN/Ag, **e** CA–MA–SA/PAN/Ag, **f** CA–PA–SA/PAN/Ag, **g** LA–MA–PA/PAN/Ag, **h** LA–MA–SA/PAN/Ag, **i** LA–PA–SA/PAN/Ag, and **j** MA–PA–SA/PAN/Ag
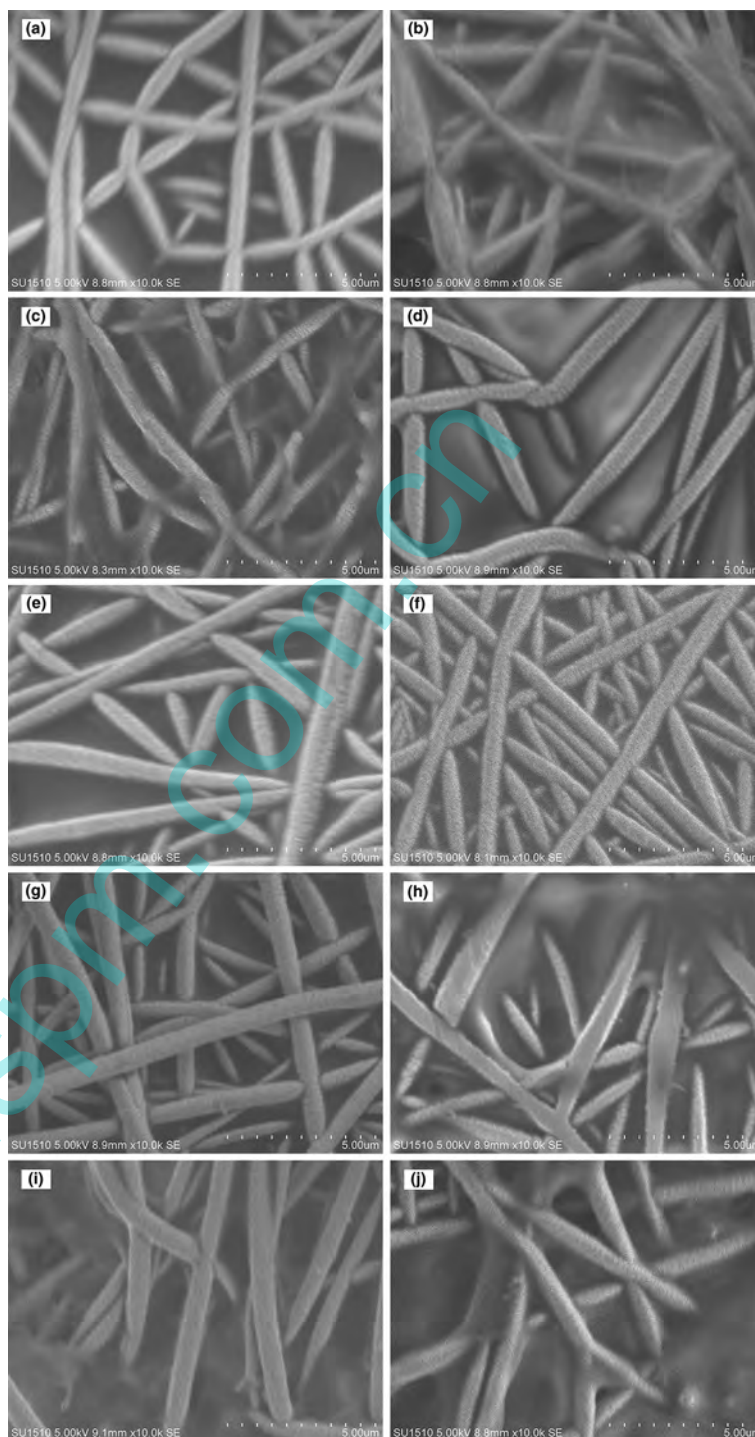
170.3 kJ kg^{-1}, respectively, indicating that the selectable phase change temperature range of practical application was effectively extended. The DSC results also revealed that preparing fatty acid eutectics was a simple and effective way to adjust the phase change temperatures of fatty acids for the lower-temperature thermal storage applications and buildings energy managements.

Thermal energy storage and release properties of composite PCMs

The DSC curves of the prepared series of form-stable composite PCMs consisting of ternary fatty acid eutectics and electrospun PAN nanofibrous mats before and after sputter coating of Ag are shown in Figs. 11 and 12. The

corresponding data of thermal properties are also listed in Table 4. As presented in Figs. 11 and 12, the different kinds of ternary fatty acid eutectics/PAN and ternary fatty acid eutectics/PAN/Ag composite PCMs all showed the single melting and freezing peaks. Additionally, the different types of composite PCMs showed different thermal energy storage and release properties, which were similar to those of corresponding ternary fatty acid eutectics. It can be found from Table 4 that the enthalpies of melting and crystallization of the ternary fatty acid eutectics/PAN/Ag composite PCMs were slightly lower than those of ternary fatty acid eutectics/PAN composite PCMs, which can be attributed to the fact that the percentage of supporting materials in composite PCMs slightly increased due to the combination of Ag nanoparticles, and the adsorbing quantities of Ag-coated PAN nanofibrous mats to ternary fatty acid eutectics slightly decreased because pore sizes of nanofibrous mats obviously declined owing to the augment of average fiber diameter after sputter coating of Ag. But phase change enthalpies of ternary fatty acid eutectics/PAN/Ag composite PCMs still retained the adequate values for thermal energy storage. As shown in Table 4, there was no significant effect on the phase change temperatures of the composite PCMs by combining Ag nanolayers into phase change systems.

Figure 13 shows that the DSC curves of the CA–LA–MA/PAN/Ag form-stable composite PCMs after 100 times thermal cycling were similar to that of composite PCMs without thermal cycling in shape. The intensity of endothermic and exothermic peaks of the prepared CA–LA–MA/PAN/Ag composite PCM can be well repeated during 100 times testing processes. In other word, there were no significant changes in the phase change temperatures and enthalpies of composite nanofibers after a certain number of thermal cycles. Based on the DSC analyses, it can be
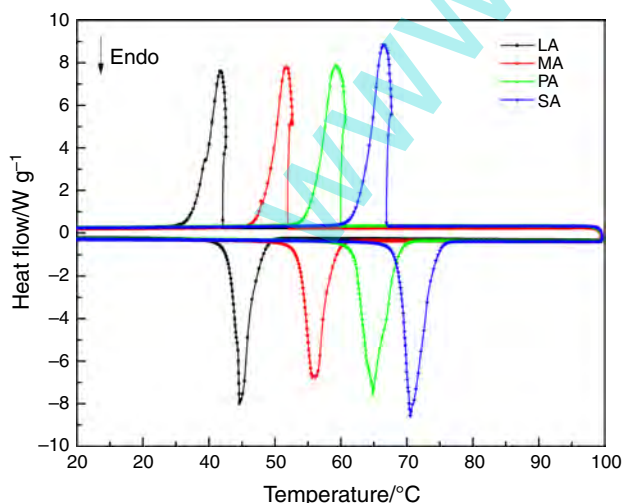

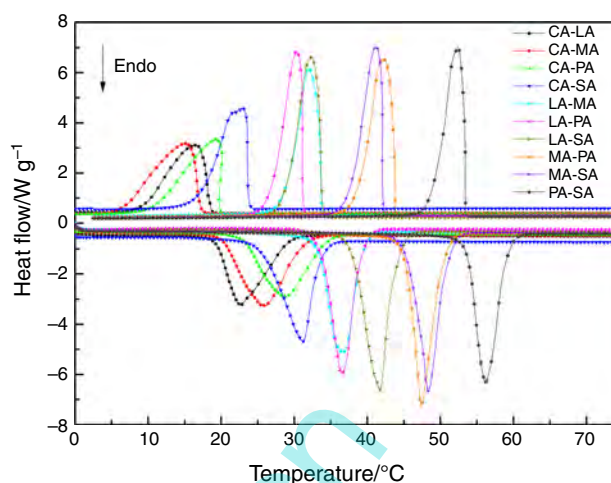**Fig. 8** DSC curves of the five fatty acids during melting and freezing processes

Fig. 9 DSC curves of the ten binary fatty acid eutectics during melting and freezing processes
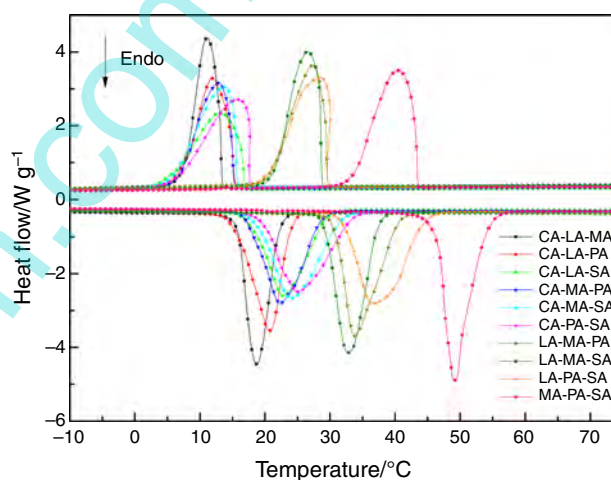

Fig. 10 DSC curves of the ten ternary fatty acid eutectics during melting and freezing processes

concluded that the prepared ternary fatty acid eutectics/PAN/Ag composite PCMs processed excellent thermal energy storage and release properties, as well as good thermal reliability.

Adsorption rates of uncoated and Ag-coated electrospun PAN nanofibrous mats

Obviously, it is important to determine the adsorption rates of the ternary fatty acid eutectics in uncoated and Ag-coated electrospun PAN nanofibrous mats, which can be calculated by the following equation:

$$\text{Adsorption rates} = (H/H_0) \times 100\%$$

where H_0 is the melting or freezing enthalpy of ternary fatty acid eutectics (see Table 3), and H is the melting or

freezing enthalpy of corresponding composite PCMs (see Table 4). The calculated adsorption rates are summarized in Table 4. It can be found that the absorption capacities of the Ag-coated PAN nanofibrous mats to ternary fatty acid eutectics are slightly lower than those of uncoated PAN nanofibrous mats. The reasons were same as previous interpretation. The growth of average fiber diameter, the decrease in pore sizes of nanofibrous mats, as well as the increase in mass present of supporting materials in composite PCMs all led to the reduction in absorption rates. In spite of this, the enthalpy efficiencies of composite PCMs still can reach about 90 %. Therefore, it was fairly easy to adsorb ternary fatty acid eutectics into the three-dimensional porous network structures of uncoated and Ag-coated PAN nanofibrous mats due to high surface-to-volume ratio, the effects of capillary force and surface tension of nanofibers membranes.

Thermal energy storage and release rates

Thermal energy storage and release rates are important thermal properties of form-stable PCMs in practical application. It is well known that fatty acid eutectics belonging to organic solid–liquid PCMs suffer from poor thermal conductivity, which would decline the heat transfer efficiencies of thermal storage systems. In this paper, the influence of the Ag nanostructured layers on the thermal energy storage and release rates of composite PCMs were also determined. The melting and freezing testing temperatures were recorded between −5 and 35 °C. Figure 14 shows the typical heating and cooling temperature–time curves of CA–LA–MA/PAN and CA–LA–MA/PAN/Ag form-stable composite PCMs. It can be seen from Fig. 14 that there was a substantial rise in the heat storage and
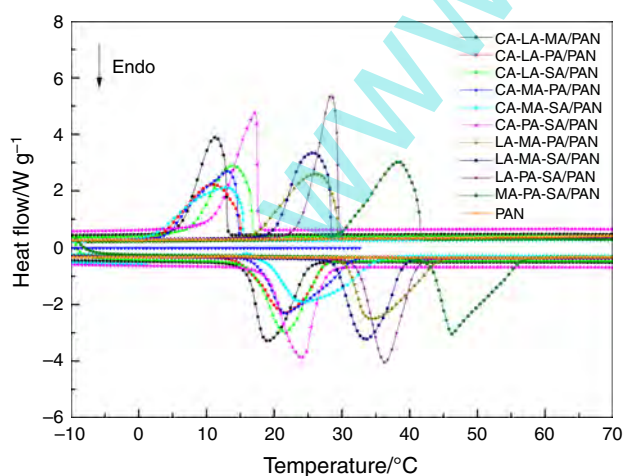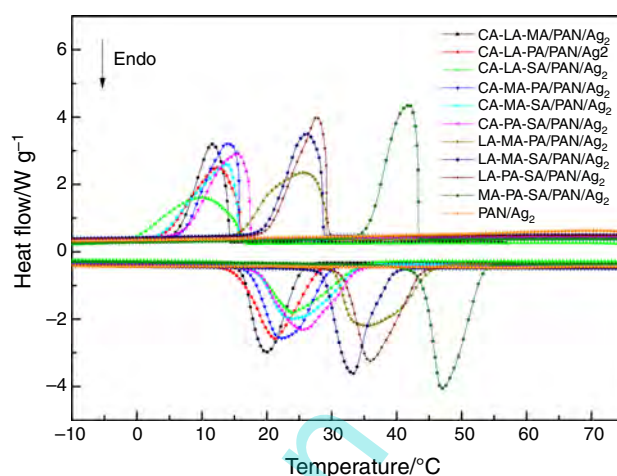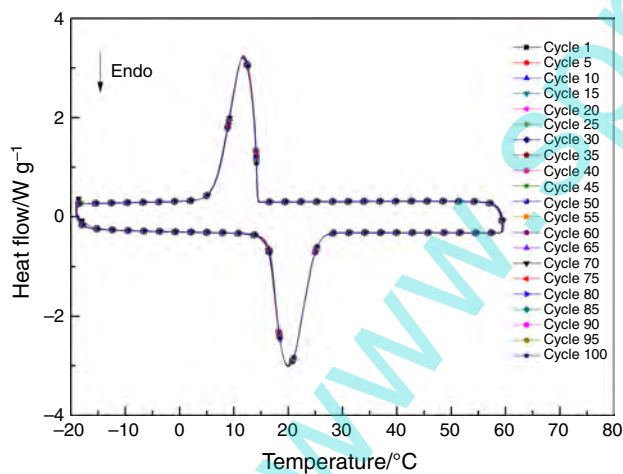
Fig. 12 DSC curves of Ag-coated PAN nanofiber membrane and the different kinds of ternary fatty acid eutectics/PAN/Ag form-stable composite PCMs

release rates of CA–LA–MA/PAN form-stable composite PCMs due to the combination of Ag nanolayers into phase change system. It was noteworthy that the corresponding melting and freezing times were, respectively, reduced about 31 and 25 % for CA–LA–MA/PU/Ag form-stable composite PCMs as compared to those of the composite PCMs without sputter coating of Ag. These decreases in melting and freezing times confirmed the improvement in thermal transfer rates of the form-stable composite PCMs after the introduction of the Ag nanolayers. Additionally, these results also indicated that the electrospun Ag-coated PAN nanofibrous mats were appropriate for acting as supporting materials to improving the thermal energy storage and release rates of phase change systems, due to the fact that the continuous thermal conducting network could be formed because Ag nanoparticles could be uniformly deposited onto the surface of electrospun nanofibrous mats to create the uniform and compact Ag nanolayers by sputter coating. These Ag nanolayers could also be seen as heat conductive bridges, which significantly contributed to form an efficient percolating path for heat flow in the ternary fatty acid eutectics/PAN form-stable composites PCMs, finally resulting in the drop of melting and freezing times. Additionally, it was clear that the pore size of PAN nanofibrous membranes significantly decrease due to the sputter Ag covered on the nanofiber surface, which led to that the mass of the adsorbed ternary fatty acid eutectics slightly declined in the same membrane volume. In other word, ternary fatty acid eutectics can be divided and dispersed into smaller network cells when Ag-coated PAN nanofibrous membranes were selected as supporting materials, which made the ternary fatty acid eutectics have more contact areas with Ag nanoparticles. The high thermal conductivity of Ag nanoparticles covering on the

Fig. 11 DSC curves of electrospun PAN nanofiber membrane and the different kinds of ternary fatty acid eutectics/PAN form-stable composite PCMs

Table 4 Adsorption rates, peak onset temperature (T_e), melting peak temperature (T_m), freezing peak temperature (T_c), melting enthalpy (ΔH_m) and freezing enthalpy (ΔH_c) of form-stable composite PCMs

Composite PCMs	Adsorption rates/%	Melting			Freezing		
		T_e/°C	T_m/°C	ΔH_m/kJ kg^{-1}	T_e/°C	T_c/°C	ΔH_c/kJ kg^{-1}
CA–LA–MA/PAN	97.11	16.06	19.11	127.6	13.04	11.33	125.9
CA–LA–MA/PAN/Ag	93.68	16.20	19.87	123.1	14.29	11.63	121.5
CA–LA–PA/PAN	93.88	16.10	21.71	125.8	15.29	10.94	121.1
CA–LA–PA/PAN/Ag	91.79	15.87	21.39	123.0	16.09	12.39	120.4
CA–LA–SA/PAN	95.77	16.84	21.76	126.9	16.94	13.90	125.5
CA–LA–SA/PAN/Ag	92.15	17.56	24.00	122.1	16.48	10.04	119.8
CA–MA–PA/PAN	96.93	17.66	21.66	132.6	14.77	13.13	130.5
CA–MA–PA/PAN/Ag	95.47	17.49	22.29	130.6	15.76	13.76	128.1
CA–MA–SA/PAN	95.27	18.49	24.35	139.0	15.43	12.94	135.1
CA–MA–SA/PAN/Ag	89.44	18.32	23.85	130.5	15.65	13.74	130.9
CA–PA–SA/PAN	95.12	19.10	24.06	138.6	17.50	17.17	137.4
CA–PA–SA/PAN/Ag	93.00	18.77	25.61	135.5	17.52	15.49	135.3
LA–MA–PA/PAN	98.07	30.64	34.39	152.7	29.50	26	151.8
LA–MA–PA/PAN/Ag	96.34	30.34	35.36	150.0	29.20	25.56	149.3
LA–MA–SA/PAN	97.06	28.97	33.48	148.4	28.44	25.76	148.6
LA–MA–SA/PAN/Ag	94.90	28.74	33.26	145.1	28.70	26.14	145.2
LA–PA–SA/PAN	96.79	32.33	36.36	153.9	29.48	28.39	152.4
LA–PA–SA/PU/Ag	95.53	31.97	35.98	151.9	29.25	27.67	150.5
MA–PA–SA/PU	97.77	43.10	46.21	166.5	41.63	38.24	166.0
MA–PA–SA/PU/Ag	96.30	44.06	47.09	164.0	43.38	42.07	164.8

Fig. 13 Typical DSC cycle curves of CA–LA–MA/PAN/Ag form-stable composite PCM

nanofibers surface allowed heat transfer throughout composite PCMs rapidly. The ternary fatty acid eutectics dispersing outer side of each network cells (i.e., each pore) of Ag-coated PAN nanofibrous membranes melt first. And then the heat can be more quickly transferred from outer side of each pore to inside of ternary fatty acid eutectics due to the smaller pore size. It is worth to point out that the most of the pores in electrospun nanofibrous membranes were interconnected, resulting in that it would be easily saturated with melted ternary fatty acid eutectics. Therefore, the decrease in pore size of Ag-coated nanofibrous membranes also played a key role in improving the heat transfer rates of the composite phase change system. It was also concluded that the magnetron sputtering technology can be used as an effective method to improve the thermal energy storage and retrieval rates of the composite PCMs.

Conclusions

In the present work, a series of ternary fatty acid eutectics acting as solid–liquid PCMs were successfully prepared according to the lowest eutectic point theory. Subsequently, the Ag-coated PAN nanofibrous mats with excellent thermal conductivity were also fabricated and selected as the supporting skeleton to absorb the prepared ternary fatty acid eutectics through effects of capillary, physical surface tension forces and nanoconfinement. The EDX results confirmed the successful deposition of Ag nanolayers on the surface of electrospun PAN nanofibers. The observations by SEM and AFM revealed that the surface of PAN nanofibers exhibited roughness structure
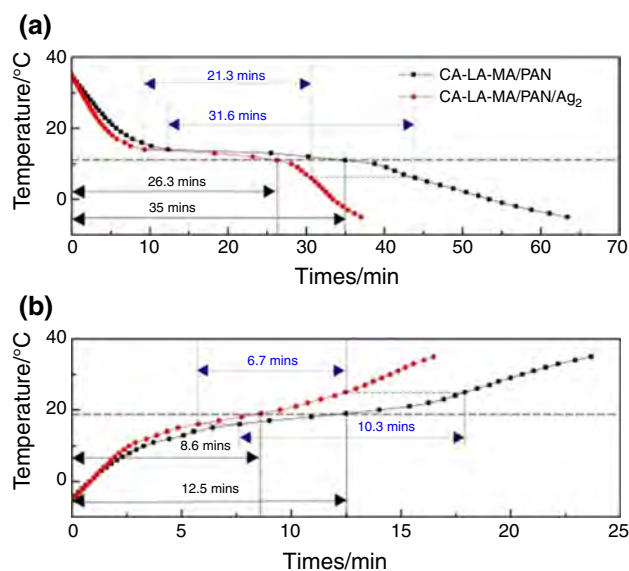
Fig. 14 Representative heat storage and release curves of CA–LA–MA/PAN and CA–LA–MA/PAN/Ag form-stable composite PCMs: **a** heat storage and **b** heat release

after magnetron sputtering of Ag. The average size of the sputtered Ag clusters was about 45 nm. The prepared ternary fatty acid eutectics/PAN/Ag form-stable composite PCMs possessed desired morphological structure, which effectively solved the leakage problem of eutectics. The DSC curves suggested that phase change temperatures of fatty acids could be effectively adjusted to the values of actual climatic requirements by preparing the ternary fatty acid eutectics. The maximum melting enthalpies of the ternary fatty acid eutectics/PAN/Ag form-stable composite PCMs amounted to 164.8 kJ kg^{-1} and the phase change temperature can be tailored in the range of −0.95 to 53.15 °C, which were suitable for the applications of lower-temperature thermal energy storage and retrieval. The melting and freezing times of ternary fatty acid eutectics/PAN/Ag form-stable composite PCMs significantly decreased about 31 and 25 % due to the introduction of functional Ag nanolayers. It was concluded that magnetron sputter is a simple and effective way to improve thermal energy storage and release rates of phase change systems.

References

1. Shukla A, Buddhi D, Sawhney RL. Solar water heaters with phase change material thermal energy storage medium: a review. Renew Sustain Energy Rev. 2009;13:2119–25.
2. Nithyanandam K, Pitchumani R, Mathur A. Analysis of a latent thermocline storage system with encapsulated phase change materials for concentrating solar power. Appl Energy. 2014;113:1446–60.
3. Zhou D, Zhao CY, Tian Y. Review on thermal energy storage with phase change materials (PCMs) in building applications. Appl Energy. 2012;92:593–605.
4. Cheng WL, Yuan XD. Numerical analysis of a novel household refrigerator with shape-stabilized PCM (phase change material) heat storage condensers. Energy. 2013;59:265–76.
5. Jankowski NR, McCluskey FP. A review of phase change materials for vehicle component thermal buffering. Appl Energy. 2014;113:1525–61.
6. Goli P, Legedza S, Dhar A, Salgado R, Renteria J, Balandin AA. Graphene-enhanced hybrid phase change materials for thermal management of Li-ion batteries. J Power Sources. 2014;248:37–43.
7. Kandasamy R, Wang XQ, Mujunidar AS. Application of phase change materials in thermal management of electronics. Appl Therm Eng. 2007;27:2822–32.
8. Ozturk HH. Experimental evaluation of energy and energy efficiency of a seasonal latent heat storage system for greenhouse heating. Energy Convers Manag. 2005;46:1523–42.
9. Onder E, Sarier N, Cimen E. Encapsulation of phase change materials by complex coacervation to improve thermal performances of woven fabrics. Thermochim Acta. 2008;467: 63–72.
10. Regin AF, Solanki SC, Saini JS. Heat transfer characteristics of thermal energy storage system using PCM capsules: a review. Renew Sustain Energy Rev. 2008;12:2438–58.
11. Zeng JL, Sun LX, Xu F, Tan ZC, Zhang ZH, Zhang J, Zhang T. Study of a PCM based energy storage system containing Ag nanoparticles. J Therm Anal Calorim. 2007;87:369–73.
12. Zeng JL, Zhang J, Liu YY, Cao ZX, Zhang ZH, Xu F, Sun LX. Polyaniline/1-tetradecanol composites form-stable PCMS and electrical conductive materials. J Therm Anal Calorim. 2008;91:455–61.
13. Sari A. Eutectic mixtures of some fatty acids for latent heat storage: thermal properties and thermal reliability with respect to thermal cycling. Energy Convers Manag. 2006;47:1207–21.
14. Sharma A, Shukla A, Chen CR, Dwivedi S. Development of phase change materials for building applications. Energy Build. 2013;64:403–7.
15. Yuan YP, Zhang N, Tao WQ, Cao XL, He YL. Fatty acids as phase change materials: a review. Renew Sustain Energy Rev. 2014;29:482–98.
16. Mngomezulu ME, Luyt AS, Krupa I. Structure and properties of phase-change materials based on high-density polyethylene, hard Fischer–Tropsch paraffin wax, and wood flour. Polym Compos. 2011;32:1155–63.
17. Cai YB, Song L, He QL, Yang DD, Hu Y. Preparation, thermal and flammability properties of a novel form-stable phase change materials based on high density polyethylene/poly(ethylene-co-vinyl acetate)/organophilic montmorillonite nanocomposites/paraffin compounds. Energy Convers Manag. 2008;49:2055–62.
18. Zhu FR, Zhang L, Zeng JL, Zhu L, Zhu Z, Zhu XY, Li RH, Xiao ZL, Cao Z. Preparation and thermal properties of palmitic acid/polyaniline/copper nanowires form-stable phase change materials. J Therm Anal Calorim. 2014;115:1133–41.

19. Cai YB, Gao CT, Zhang T, Zhang Z, Wei QF, Du JM, Hu Y, Song L. Influences of expanded graphite on structural morphology and thermal performance of composite phase change materials consisting of fatty acid eutectics and electrospun PA6 nanofibrous mats. Renew Energy. 2013;57:163–70.

20. Chen CZ, Wang L, Huang Y. Morphology and thermal properties of electrospun fatty acids/polyethylene terephthalate composite fibers as novel form-stable phase change materials. Sol Energy Mater Sol Cells. 2008;92:1382–7.

21. Harikrishnan S, Magesh S, Kalaiselvam S. Preparation and thermal energy storage behaviour of stearic acid-TiO2 nanofluids as a phase change material for solar heating systems. Thermochim Acta. 2013;565:137–45.

22. Chen Z, Shan F, Cao L, Fang GY. Synthesis and thermal properties of shape-stabilized lauric acid/activated carbon composites as phase change materials for thermal energy storage. Sol Energy Mater Sol Cells. 2012;102:131–6.

23. Fang XM, Zhang ZG, Chen ZH. Study on preparation of montmorillonite-based composite phase change materials and their applications in thermal storage building materials. Energy Convers Manag. 2008;49:718–23.

24. Li M, Kao HT, Wu ZS, Tan JM. Study on preparation and thermal property of binary fatty acid and the binary fatty acids/diatomite composite phase change materials. Appl Energy. 2011;88:1606–12.

25. Tang BT, Agi JS, Wang YM, Jia C, Zhang SF. Facile synthesis and performances of PEG/SiO$_2$ composite form-stable phase change materials. Sol Energy. 2013;97:484–92.

26. Wei T, Zheng BC, Liu J, Gao YF, Guo WH. Structures and thermal properties of fatty acid/expanded perlite composites as form-stable phase change materials. Energy Build. 2014;68:587–92.

27. Mehrali M, Latibari ST, Mehrali M, Mahlia TMI, Metselaar HSC, Naghavi MS, Sadeghinezhad E, Akhiani AR. Preparation and characterization of palmitic acid/graphene nanoplatelets composite with remarkable thermal conductivity as a novel shape-stabilized phase change material. Appl Therm Eng. 2013;61:633–40.

28. Zhang ZG, Zhang N, Peng J, Fang XM, Gao XN, Fang YT. Preparation and thermal energy storage properties of paraffin/expanded graphite composite phase change material. Appl Energy. 2012;91:426–31.

29. Wei QF, Wang XQ, Gao WD. AFM and ESEM characterisation of functionally nanostructured fibres. Appl Surf Sci. 2004;236:456–60.

30. Wei QF, Wang YY, Wang XQ, Huang FL, Yang SW. Surface nanostructure evolution of functionalized polypropylene fibers. J Appl Polym Sci. 2007;106:1243–7.

31. Wang XF, Ding B, Sun G, Wang M, Yu J. Electro-spinning/netting: a strategy for the fabrication of three-dimensional polymer nano-fiber/nets. Prog Mater Sci. 2013;58:1173–243.

32. Yarin AL, Kataphinan W, Reneker DH. Branching in electro-spinning of nanofibers. J Appl Phys. 2005;98:064501.

33. Ke HZ, Pang ZY, Xu YF, Chen XD, Fu JP, Cai YB, Huang FL, Wei QF. Graphene oxide improved thermal and mechanical properties of electrospun methyl stearate/polyacrylonitrile form-stable phase change composite nanofibers. J Therm Anal Calorim. 2014;117:109–22.

34. Ma GP, Yang DZ, Nie J. Preparation of porous ultrafine polyacrylonitrile (PAN) fibers by electrospinning. Polym Adv Technol. 2009;20:147–50.